Research Square

Preprints are preliminary reports that have not undergone peer review.
They should not be considered conclusive, used to inform clinical practice,
or referenced by the media as validated information.

Dielectric Behaviour of Acrylic and Natural Rubber Dielectric Elastomers: Combined Effects of Frequency, Temperature and Mechanical Pre-stretch

Ajeet Kumar

ajeet.pme15@iitp.ac.in

Galgotias University

Anjani Kumar

Government Engineering College

Abhishek Kumar Shukla

Galgotias University

Md Shamim Shah

Zeal College of Engineering and Research

Research Article

Keywords: Dielectric constant, Electroactive polymers, Soft robotics, Optimal range

Posted Date: September 9th, 2026

DOI: https://doi.org/10.21203/rs.3.rs-10792848/v1

License: This work is licensed under a Creative Commons Attribution 4.0 International License.
Read Full License

Additional Declarations: No competing interests reported.

Dielectric Behaviour of Acrylic and Natural Rubber Dielectric Elastomers: Combined Effects of Frequency, Temperature and Mechanical Pre-stretch

Ajeet Kumar[a,b,*], Anjani Kumar[c], Abhishek Kumar Shukla[a], Md Shamim Shah[d]
[a]Department of Mechanical Engineering, Galgotias University, Greater Noida, India-203201
[b]Department of Mechanical Engineering, Indian Institute of Technology Patna, Bihar, 801103, India
[c]Department of Mechanical Engineering, Government Engineering College, Arwal-804409, Bihar, India

[d]Department of Robotics and Automation, Zeal College of Engineering and Research, Nrahe, Pune 411041, India

[*]Corresponding author
Email addresses: ajeet.pme15@iitp.ac.in (Ajeet Kumar),

Abstract

Dielectric properties determine the electromechanical response of electroactive polymer (EAP) actuators and the conversion efficiency of EAP generators. The dielectric constant is especially critical, since it directly governs how effectively such sensors, actuators, and generators perform. The present work compares how frequency, temperature, and mechanical pre-stretch jointly affect the dielectric constants of two candidate elastomers: acrylic VHB 4910 and natural rubber Oppoband 8001. Measurements spanned 1 Hz to 1 MHz across temperatures from −80°C to 60°C, with biaxial pre-stretch states ranging from $\lambda_1 \times \lambda_2$ = 1×2 to 3×4. In both elastomers, the dielectric constant fell as frequency rose and as temperature moved away from the optimum, a consequence of dielectric relaxation, and declined steadily with increasing pre-stretch owing to restricted dipole reorientation. VHB 4910 proved considerably more sensitive, its permittivity dropping by 32.53% at 0°Ccompared with only 14.23% for Oppoband 8001, a difference traceable to the contrasting polarity of the two polymer backbones. Fitting the measurements to the Debye model and to a combined pre-stretch–temperature expression yielded glass transition temperatures of −42℃ and −68℃, respectively. These results define operational temperature limits that can inform material selection, particularly for soft robotic applications.

Keywords: Dielectric constant, Electroactive polymers, Soft robotics, Optimal range.

1. Introduction

Electroactive polymers are the type of 4D smart material that change their size and shape when stimulated in the presence of an electric field and vice versa [1–7].Due to its promising features such as high energy density, high reliability, better recyclability, high efficiency and low cost, etc, dielectric elastomer could be used in vast applications i.e., in actuator [8–12], soft robotics [13], micro air vehicle [13], adaptive devices [14], prosthetic devices [15], braille display [16], dielectric elastomer generators [17, 18]. Among different applications, a dielectric elastomer actuator is one of the most promising. An external electric field is applied through complaint electrodes coated from both sides on a thin dielectric elastomer film. The electrostatic pressure is built up due to an electric field that compels the elastomer film to compress in the thickness direction and expand in the lateral direction [19]. The electrostatic pressure ‘P’, also known as Maxwell stress, is given by equation (1).

$$P = \varepsilon_0 \varepsilon_r \left(\frac{V}{d}\right)^2 \quad (1)$$

where, ε_0 represents the permittivity of free space, ε_r represents the relative permittivity or dielectric constant, V is the applied voltage on the electrode, d is the thickness of dielectric elastomer film [20].

The performance of the dielectric elastomer actuator highly depends upon the dielectric constant considered in equation (1). The dielectric constant is represented as a complex function due to delay in dielectric polarization with change in electric field as

$$\epsilon = \epsilon' - j\epsilon'' = |\epsilon| e^{-j\delta} \quad (2)$$

where, ϵ' is the dielectric constant, ϵ'' is the dielectric loss factor, and δ is the dielectric loss angle [21]. Further, the loss tangent, i.e., the dissipation factor, is given by equation (3), which is proportionally related to the waste energy per cycle [22].

$$\tan\delta = \frac{\epsilon''}{\epsilon'} \quad (3)$$

The dielectric constant is not a fixed property; rather, it is sensitive to a range of operational parameters, including frequency [23], temperature [24], and mechanical pre stretching [25]. These dependencies can introduce dielectric relaxation effects that degrade device performance, especially under dynamic conditions [26]. For example, temperature-induced molecular mobility affects dipolar orientation, while increasing frequency can suppress dielectric polarization, leading to a decrease in ϵ'. Similarly, mechanical pre-stretch alters polymer chain alignment and free volume, modifying dielectric behavior [27]. Researchers have conducted limited studies on the impact of aforementioned factors on the dielectric constant. For example, Wissler et al. [28] indicated a dielectric constant value of 4.68 for VHB 4910 at 100 Hz using gold electrodes. In a study by Trols et al. [29], a dielectric constant of 4.24 at 1 Hz was experimentally determined. This was achieved by using a silver paste-compliant electrode on VHB from both sides of the film. Also, In one study, Mistral et al. [30] found that the dielectric constant of VHB at 0.1 Hz was determined to be 5.4. This measurement was obtained using carbon grease as a compliant electrode. Apart from VHB, natural rubber is another type of dielectric elastomer with promising features for dielectric elastomer applications [31–34]. However, few works have focused on the impact of various parameters such as frequency, temperature, and prestretch on the dielectric properties. Vertechy et al. [35] investigated the impact of prestretch on the dielectric constant of TheraBand™, one of the commercially available natural rubbers. They observed a negligible change in the dielectric constant, which remained at 2.7 when stretched. Furthermore, in a different study, when using a brass

electrode, they observed a decrease in dielectric constant from 2.7 to 1.3 for a prestretch value of 1 to 3, respectively. Chen et al. [36] conducted a study on the dielectric constant of two different commercially available natural rubber brands: TheraBand™ and Oppoband 8003. Their research focused on the impact of pre-stretch on the dielectric constant and found that there was not a significant change in the dielectric constant with an increase in pre-stretch. Wang and Yang [37] synthesized a methyl vinyl silane elastomer and analyzed its dielectric properties. This included examining the dielectric constant, loss, conductivity, and capacitance under various conditions. They discovered that there was minimal voltage effect on the dielectric properties. Moreover, they observed increased conductivity at frequencies above 103 Hz and better performance when using composite electrodes. Furthermore, they found that reducing the thickness in EAPs with a gold electrode led to decreases in both dielectric constant and loss. In a different study Chen et al. [38] created a machine-learning model to predict the dielectric constants of dielectric elastomers across a broad frequency range. The model effectively predicted the dielectric constants for numerous potential polymers and identified five polymers suitable for use in capacitors and microelectronics. Liu et al. [39] presented a new model for the dielectric constant of elastomers, dependent on temperature and stretch. They investigated that the stability of dielectric elastomers increases with increasing temperatures and decreasing stretch ratios. Zhang et al. [40] compared the mechanical and electrical properties of four common dielectric elastomers: PDMS, TPU, PVDF, PE and PDMS [41] has the best operating stability and electromechanical sensitivity, while TPU and PVDF have higher permittivity but suffer from poor stability due to temperature sensitivity.

Numerous researchers have explored the dielectric constant using different electrodes, but none have examined the impact of temperature, frequency, and pre-stretch on the dielectric constant of dielectric elastomers. This study is a comparative investigation of the combined effect of temperature and frequency, providing valuable insight into the extensive temperature and frequency range relevant to dielectric elastomer applications. Additionally, it pioneers an examination of the influence of pre-stretch on the dielectric constant of dielectric elastomers, marking a significant contribution to the field. The study utilized an acrylic elastomer (VHB 4910), Oppoband 8001 (yellow), a commercially available natural rubber, to explore the effects of various stretching configurations, as well as a wide range of frequencies and temperatures on the dielectric properties of these elastomers.

2. Material Details and Experiments

2.1. Materials

This research examined two varieties of dielectric elastomers utilised as Electroactive Polymers (EAPs): an acrylic-based substance known as VHB 4910 and natural rubber Oppoband 8001. The acrylic version, VHB 4910, possesses a thickness of 1 mm. This research examined two varieties of dielectric elastomers utilised as Electroactive Polymers (EAPs): an acrylic-based substance known as VHB 4910 and natural rubber Oppoband 8001. The acrylic version, VHB 4910, possesses a thickness of 1 mm.

Exceptional Bond adhesive tape produced by the American firm 3M. It is categorised as an alkyl acrylate copolymer, and its precise chemical formulation is proprietary. Conversely, the Oppoband 8001 is a fitness resistance band fabricated from natural rubber (latex), designed for physical rehabilitation purposes and produced by Oppo Medical Inc. In our research, Oppoband 8001 is distinguished as the slimmest alternative, measuring merely 150 μm in thickness. Table 1 presents comprehensive specifications of various elastomers, encompassing kind, commercial designation, electrode composition, and thickness. Both substances employ carbon conductive grease (MG Chemicals) as their electrode medium, with the acrylic and natural rubber having thicknesses of 1 mm and150 μm, respectively, demonstrating their appropriateness for various EAP applications.

Table 1

2.2. Preparation of pre-stretched elastomer films for dielectric constant measurement

This study employed both biaxial and uniaxial deformation modes, which are standard practices for testing rubber materials [42]. The biaxial stretching allowed us to independently manipulate the planar stretches, λ_1 and λ_2 to achieve a wide range of stretch combinations on the elastomers. This was facilitated by a custom-built stretching device, depicted in Figure 1, equipped with four arms for stretching and another four for stretch limitation. Each arm designed for stretching is connected at one end to the material being tested and, at the other end, to a stretch-limiting arm once the desired extension is achieved. The latter features holes aligned with predetermined stretch levels, into which pins at the stretching arms' ends are inserted to secure the stretched material. For VHB elastomers, the inherent tackiness of the material eliminates the need for external adhesives for attachment to the frame. In contrast, the non-adhesive Oppoband samples are affixed to the stretching mechanism using Polyfix glue to ensure proper fixing and stability during testing.

2.3. Measurements Conditions

Across all modes of stretching for both materials, a total of 132 samples were tested, highlighting the comprehensive nature of this study. Three primary experimental variables temperature, frequency, and mechanical prestretch were systematically changed to assess their singular and interactive influences on the dielectric characteristics of the studied dielectric elastomers. Of the configurations listed in Table 2, the unequal-biaxial states spanning $\lambda_1 \times \lambda_2 = 1 \times 2$ to 3×4 are reported in detail in Section 3.3, as these provided the widest continuous range of the stretch product across both materials. Dielectric properties characterization was carried out under different parameters utilised in this research as outlined:

1. Temperature: The dielectric response influenced by temperature was examined throughout an extensive thermal range to identify variations in molecular mobility, polarisation processes, and dielectric relaxation characteristics. Measurements for VHB 4910 were taken from -60℃ to

60°C, while Oppoband 8001 was assessed in a broader spectrum of −80°Cto 60°C. In both studies, the reduced experimental temperatures were chosen to fall beneath their corresponding glass-transition temperatures, facilitating the examination of the dielectric response inside the glassy and transition phases.

2. Frequency: The dielectric properties dependent on frequency were assessed across a significantly wide frequency range from 1 Hz to 10 MHz. This spectrum includes low-frequency interfacial and dipolar polarisation mechanisms alongside high-frequency molecular and electronic polarisation responses, facilitating a systematic evaluation of dielectric relaxation processes.
3. The influence of mechanical pre-stretch on the dielectric constant was examined by exposing the elastomer samples to various regulated deformation conditions. Equal-biaxial, unequal-biaxial, and pure-shear stretching configurations were applied to represent diverse states of mechanical constraint and anisotropy. The applied pre-stretch alters the polymer-chain arrangement, specimen thickness, molecular orientation, and electromechanical coupling characteristics, which can consequently modify the effective dielectric constant. The corresponding deformation ratios and stretching conditions for each configuration were methodically defined, and their specifics are summarized in Table 2. This parametric analysis provides a complete framework for linking thermal, electrical, and mechanical stressors with the dielectric behaviour of elastomeric materials.

Figure 1

2.4. Dielectric constant measurement

The dielectric characteristics of the elastomeric films, such as the dielectric constant and dielectric loss, were empirically assessed utilising a Novocontrol Spectroscopy Alpha Analyser across a frequency spectrum of 1 Hz to 1 MHz with an applied bias voltage of 1 V. The complete measurement arrangement, comprising the analyser, the temperature regulated cryostat and the liquid nitrogen Dewar, is shown in Figure 2. Before measurement, the prepared dielectric elastomer samples were placed within a temperature-regulated cryostat, ensuring a controlled measurement setting and reducing the impact of external electromagnetic interference, variations in ambient temperature, and environmental noise on the electrical response. In experiments with mechanically pre-stretched samples, the dielectric elastomer films were firmly affixed within a circular mechanical apparatus to uphold the specified pre-stretch ratio and guarantee dimensional integrity during the characterisation phase. This configuration inhibited relaxation or uneven deformation of the samples during electrical stimulation. Carbon conductive grease (MG Chemicals) was meticulously applied on both sides of each elastomer layer to ensure consistent and low-resistance

electrical connectivity while accommodating the flexible characteristics of the polymer material. Following this, circular electrodes made of gold-plated copper, each with a diameter of 20 mm, were affixed to either side of the specimen to establish a clearly defined parallel-plate electrode arrangement for dielectric analysis. The configuration of the electrodes and uniform contact area facilitated the accurate assessment of the intricate dielectric response across the examined frequency range. The electrical response obtained was further processed and examined with the WinDETA software provided by Novocontrol, from which the frequency-dependent dielectric constant and dielectric loss properties were derived. This experimental approach facilitated a methodical assessment of the effects of frequency and mechanical pre-stretch on the dielectric properties of elastomer films, while maintaining consistent and dependable measurement conditions. Each stretch and temperature condition was measured on three independently prepared specimens, and the values reported throughout Section 3 represent the mean of these three measurements. The maximum deviation between repeat specimens was within ±5%, confirming the repeatability of the measurement procedure.

Table 2

Figure 2

3. Results and Discussion

3.1. Effect of frequency on dielectric constant

Figure 3 effectively demonstrates the influence of a broad spectrum of frequencies on the dielectric constant of acrylic and natural rubber. Dielectric polarisation depends on the alternating field, specifically the frequency of the applied field. The dielectric constant diminishes as frequency increases for both substances. This is because dipoles fail to polarize due to rapid change in the field which goes on increasing with increasing frequency. In the case of VHB 4910 which is a polar rubber, the change in dielectric constant is more with increasing frequency which is due to dipole relaxation especially β-relaxations as compared to natural rubber which has low polarity hydrocarbon temperature section. Oppoband 8001 shows less decrease in dielectric constant with increasing frequency as illustrated in table 3. Conversely, the loss tangent rises with frequency at

Figure 3

ambient temperatures (20 ℃, 40 ℃, and 60 ℃) for VHB 4910, attributed to a reduction in the relaxation period for dipole polarisation. This results into increases in dielectric loss tangent as

shown in Figure 4. However, as the temperature falls below room temperature dielectric loss decreases as the dipole relaxation time increases with a decrease in room temperature. In the case of Oppoband 8001 the loss tangent is negligible with an increase in frequency which proves the absence of polar groups in natural rubber [45, 46]. However, for room temperature and above (20 ℃, 40℃, and 60℃) the alignment of the dipole increases which results in an increase in dielectric loss from 1 Hz to 100 Hz. Further, an increase in frequency results in a decrease in the alignment of dipoles as the alternating of the electric field increases.

Table 3

Figure 4

3.2. Effect of temperature on dielectric constant

Figure 5 depicts effect of temperature on dielectric constant. In case of VHB 4910 dielectric constant increases appreciably (within 1000Hz) with temperature up to 0℃ and found to be decreasing with further increase in temperature. This is because as the temperature increase from room temperature the thermal energy of molecules also increases which results into increase in amplitude of random motion of dipoles. As a result, alignment of dipoles decreases, and dielectric constant decreases. Conversely, for the frequency range of 1000 to 10000 Hz, dielectric constant also increases for temperature below 0℃. However, it remains almost constant as the temperature increases above 0℃. Further dielectric constant increases with increase in temperature for frequency above 10000 Hz. This change in dielectric constant is due to the orientation polarization of the dipoles with change in frequency and temperature simultaneously [47]. The dipole rotation results into increase or decrease of dielectric polarization which is affected by temperature as per the Debye model given in equation (4).

$$\varepsilon_r{}' = \varepsilon_\infty + \frac{N\mu^2}{3\varepsilon_0 kT} \tag{3}$$

where, μ is the dipole moment, N is the dipole density, ε_∞ is the dielectric constant at very high frequency, $\varepsilon_r{}'$ is the relative dielectric constant, ε_0 is the dielectric constant of vacuum, T is the temperature, and k is the Boltzmann constant.

Figure 5

The dielectric loss also shows similar trends with a dielectric constant of both the elastomer. Dielectric loss is minimal at a temperature below glass transition temperature (T_g) of elastomers as the mobility of dipole seizes which results in lower dissipation losses as shown in figure 6. As temperate increases above (T_g) dielectric loss increase as the mobility of dipole increases. Further

increase in temperate increases the thermal energy of dipoles which results into decrease in orientation polarization of dipole due to increase in randomness of dipoles.

Figure 6

Glass transition temperature (T_g) of the elastomers was determined by dynamic mechanical analysis (DMA), in which the damping factor (tan δ) of the elastomer is measured as a function of temperature. The temperature at which the tan δ curve reaches its peak value gives the T_g of the elastomer. Figure 7 shows the variation of tan δ with temperature for VHB 4910 and Oppoband 8001. The tan δ peaks occur at −42 ◦C and −68 ◦C, respectively, which are therefore taken as the glass transition temperatures of VHB 4910 and Oppoband 8001. The dielectric constant decreases as the temperature approaches the glass transition temperature of dielectric elastomers. This is because at the glass transition temperature, the elastomer is in a glassy phase, which resists the mobility of dipoles. As a result, the polarization of the dipole is hindered by the resistance force which resists the rotation of the dipole with the applied electric field. This is observed in both VHB 4910 and Oppoband 8001 as well, depending upon the T_g and polarity of the elastomer. Therefore, Figure 5 depicts there are decreases in the dielectric constant reported in VHB 4910 as well as Oppoband 8001.

Figure 7

In both the elastomers, as temperature increases above glass transition temperature, the dielectric constant increase. This is because dipole gets thermal energy causing decreases in the resisting force of rotation and dipole polarization increases with the applied electric field [48]. In case of VHB 4910, at 0°C dielectric constant is maximum which shows that the dipole polarization is much sensitive to the applied electric field. [49]. Further, increase in temperature causes an increase in thermal energy causing an increase in the mobility of the dipole resulting into interference in dipole polarization. Hence, the dielectric constant decreases for lower frequencies below 1000 Hz [50]. For larger frequencies above 1000 Hz, dipole polarization is fully supported with the thermal mobility of the dipole [51]. Hence, Figure 5 depicts dielectric constant increases monotonically.

Figure 8

In case of Oppoband 8001, for lower frequencies say below 100 Hz dielectric constant decreases as temperature approaches glass transition temperature ($-$ 68°C) similar to VHB 4910. As temperature increases above the glass transition temperature dielectric constant increases. On further temperature increases dielectric constant decreases with similar trends as of VHB 4910. For higher frequencies above 1000 Hz dielectric constant decreases monotonically because the thermal mobility of dipoles increases which hinders the dipole polarization. Oppoband 8001 shows different trends with VHB 4910 for higher frequency this is because natural rubber polymers have low

polarity as compared to VHB 4910 [45, 52, 53]. Figure 8 shows the Debey model fitting which considered the combined effect of temperature and frequency. The curve fitting slope for VHB 4910 is found to be more as compared to that of Oppoband 8001. This demonstrates that, in comparison to Oppoband, the dielectric constant of VHB is more temperature and frequency sensitive.

3.3. Effect of pre-stretch on dielectric constant

Figure 10 shows the combined effects of temperature and pre-stretch on the dielectric constant of VHB 4910 and Oppoband 8001 at a fixed frequency of 1 Hz. Earlier few research groups reported the decreases of dielectric constant with pre-stretch [54–56]. Nonetheless, the simultaneous impact of temperature and pre-stretch is an important aspect to be investigated. In the previous literature, the frequency-dependent dielectric constant has been reported for VHB 4910 [29, 57] but there was variation in the dielectric constant reported by the researchers. However, less variation was reported in the case of natural rubber as compared to VHB 4910 [35, 58]. Figure 9 shows the combined effects of temperature and prestretch on the dielectric constant of VHB and Oppoband at a fixed frequency of 1 Hz.

Figure 9

In both the materials there is a decrease in dielectric constant with higher pre-stretch due to the orientation polarization. In case of VHB 4910 at low frequency say at 1 Hz when there is no any effects of dielectric relaxations the dielectric constant decreases linearly from 6.27 to 4.23 at 0 °C. Similar decreasing trends are observed for all temperature ranges as shown in table 4. Pre-stretch constrain the dipoles in the polymer main chain to align with the applied electric field causing a decrease in dielectric constant. Further due to temperature which also affects the dipole polarization explained in the previous sections results in a further decline in the dielectric constant. Natural rubber strain-induced crystallization affects the dielectric constant of rubber [59, 60]. The crystallinity of natural rubber increases due to elongation in the polymer chain due to pre-stretch an increase in crystallinity results in decreases in the dielectric constant. The dielectric constant in relation to temperature and pre-stretch is effectively described by equation (5), applicable for temperatures over 0°C [61].

Figure 10 presents the variation of the dielectric constant with the biaxial pre-stretch product $\lambda_1 \times \lambda_2$ at a fixed frequency of 1 Hz, measured across the full temperature range for both elastomers. This frequency was selected because dielectric relaxation effects are absent at 1 Hz, so that the measured permittivity reflects the equilibrium orientational polarisation of the dipoles and the influence of mechanical constraint can be isolated from frequency dependent losses. In both materials the dielectric constant decreases monotonically as the pre-stretch product increases from

1×2 to 3×4, and the decreasing trend is preserved at every temperature examined, indicating that the mechanical and thermal contributions act independently over this range.

The magnitude of the reduction differs markedly between the two elastomers. For VHB 4910 the dielectric constant falls from 6.27 to 4.23 at $\lambda_1 \times \lambda_2 = 1\times2$ to 3×4 at 0°C, corresponding to a reduction of 32.53%, with the percentage change across all temperatures lying between 32.53% and 43.50%, as summarised in Table 4. In contrast, Oppoband 8001 exhibits a decrease from 2.60 to 2.23 over the same stretch range at 0°C, amounting to only 14.23%, with the reduction confined to a narrow band of 13.15% to 14.45% across the entire temperature range. VHB 4910 is therefore approximately three times more sensitive to pre-stretch than Oppoband 8001. This contrast originates in the molecular architecture of the two materials: the acrylate side groups of VHB 4910 carry permanent dipole moments that are progressively immobilised as the polymer chains align under biaxial extension, whereas the non-polar hydrocarbon backbone of natural rubber possesses few orientable dipoles, so that its permittivity is governed largely by induced polarisation and is correspondingly insensitive to chain alignment. A second mechanism contributes in the case of Oppoband 8001, namely strain-induced crystallisation, in which chain elongation under pre-stretch raises the crystalline fraction of the natural rubber and further lowers the effective dielectric constant [59, 60].

Figure 10

It is also notable that for VHB 4910 the family of curves in Figure 10 is not ordered monotonically with temperature. The highest permittivity at every stretch level is recorded at 0°C, above and below which the values decline. This is consistent with the temperature dependence established in Section 3.2, where the maximum dipole polarisation for VHB 4910 was likewise observed at 0°C. For Oppoband 8001 the curves are ordered more regularly, with permittivity decreasing progressively as temperature rises from −80°C to 60°C.

$$\varepsilon(\lambda, T) = a(\lambda_1, \lambda_2) + \frac{b}{T} + \mathrm{c} \tag{5}$$

Where, 'a' is the electrostriction constant of elastomers, 'b' is a constant expressed as $M{\eta_d}^2/3k\varepsilon_0$, here M, η_d, k, and ε_0 are dipole current density, dipole moment, Boltzmann constant and vacuum permittivity, respectively, 'c' is the dielectric constant of dielectric elastomer at a given temperature without any deformation, T is temperature in Kelvin and λ_1, λ_2 are the pre-stretch values. Curve fitting of Equation 3 is shown in Figure 8 and fitting constants are shown in Table 5.

From equation (5), the dielectric constant and temperature have an inverse relationship, which indicates that it will decrease an increase of temperature above 0°C also supported by curve fitting shown in Figure 8. The dielectric loss also decreases with increasing pre-stretch as dielectric

polarizations are constrained by mechanical stress generated due to pre-stretch in both the dielectric elastomers. In the case of VHB 4910, the dielectric loss declines more with a rise in pre-stretch as compared to Oppoband 8001 as acrylic rubbers are more polar than natural rubbers illustrated in Figure 9 [52].

3.4. Effect of pre-stretch on dielectric loss

Figure 9 presents the variation of dielectric loss with the pre-stretch product $\lambda_1 \times \lambda_2$ at 1 Hz for both elastomers across the full temperature range. In both materials, the dielectric loss decreases with increasing pre-stretch, as the mechanical stress developed under biaxial extension constrains the reorientation of the dipoles and thereby reduces the energy dissipated per cycle. The reduction is markedly steeper for VHB 4910, whose loss falls from approximately 0.048 to 0.026 at −20°C, than for Oppoband 8001, consistent with the greater polarity of the acrylate side groups relative to the non-polar hydrocarbon backbone of natural rubber [52]. For Oppoband 8001, the dielectric loss remains below 0.025 at all temperatures up to 40°C, rising appreciably only at 60°C, which indicates a wide window of low dissipation operation for this material.

3.5. Combined modelling of pre-stretch and temperature effects

Figure 11 presents the three-dimensional least-squares fitting of Eq. 5 to the measured dielectric constants, plotted as a function of the pre-stretch product $\lambda_1 \times \lambda_2$ and the reciprocal absolute temperature 1000/T. The reciprocal temperature scale is adopted because Eq. 5 is linear in 1/T, so that the model reduces to a plane in the ($\lambda_1 \times \lambda_2$, 1000/T) space and the adequacy of the description can be assessed directly from the scatter of the experimental points about that plane. The fitted range spans 1000/T ≈ 3.0 to 3.6K^{-1}, corresponding to approximately 0°C to 60°C, in accordance with the stated validity of Eq. 5 above 0°C. The discrete markers denote the measured values, while the continuous coloured surface represents the fitted response, with the constants a, b and c listed in Table 5.

Figure 11

Table 4

For both elastomers the fitted surface descends monotonically with increasing $\lambda_1 \times \lambda_2$ at any fixed temperature, confirming the negative sign of the electrostriction constant ‘a’ and reflecting the constraint imposed on dipole reorientation by biaxial extension. Along the reciprocal temperature axis the surface rises with increasing 1000/T, that is, with decreasing absolute temperature, confirming the inverse relationship between dielectric constant and temperature embodied in the ‘b/T’ term. The magnitudes of the fitting constants quantify the contrast already evident in Figure

11. The electrostriction constant for VHB 4910 is ‘a’ = −0.0410 against −0.0265 for Oppoband 8001, indicating a steeper decline with pre-stretch, while the temperature coefficient is ‘b’ = 603 for VHB 4910 against 452 for Oppoband 8001, indicating a stronger thermal dependence. The undeformed baseline permittivity ‘c’ is 3.610 for VHB 4910 and 1.529 for Oppoband 8001, consistent with the substantially higher polarity of the acrylic elastomer. The essentially planar form of both fitted surfaces further indicates that, over the ranges examined, the contributions of pre-stretch and temperature are additive rather than coupled, so that Eq. 5 provides an adequate phenomenological description of the combined influence of mechanical and thermal loading on the permittivity of both dielectric elastomers.

Table 5

3.6. Operational temperature range for material selection

The combined dielectric-constant and loss data allow a practical operating window to be defined for each elastomer. For VHB 4910, the dielectric constant attains its maximum of 5.84 at 0°C and 1 Hz, while the loss tangent remains below 0.05 between −20°C and 20°C. Below −20°C, the approach to the glass transition at −42°C suppresses dipole mobility and the permittivity falls sharply, whereas above 20°C the loss tangent rises rapidly, reaching 0.087 at 40°C and 105 Hz. VHB 4910 is therefore best employed between approximately −20°C and 20°C, where high permittivity coincides with acceptable dissipation. Oppoband 8001, by contrast, exhibits a lower but far more stable permittivity, varying by less than 6% between −80°C and 40°C, with the loss tangent remaining negligible until 60°C. Natural rubber is consequently the preferable choice for applications demanding thermal stability over a wide range, while the acrylic elastomer is preferable where maximum permittivity is required within a narrow, near-ambient temperature band.

4. Conclusions

Comprehensive experimental analysis of dielectric elastomers subjected to diverse external factors, such as frequency, temperature, and mechanical pre-stretch, yields a detailed and systematically arranged repository for comprehending their dielectric behaviour and enhancing their prospective uses in soft electromechanical systems. The collective impact of these factors is crucial, as the dielectric constant is determined by molecule polarisation, segmental mobility, chain alignment, and structural changes in the elastomer matrix. The experimental findings suggest that beta-relaxation is essential in polar dielectric elastomers with polar side-chain groups, especially in influencing the dielectric response that varies with frequency and temperature. As temperature rises, increased molecule mobility determines the relaxation dynamics, while changes in excitation

frequency limit the degree to which various polarisation mechanisms can react to the applied electric field. Mechanical pre-stretching imparts an additional structural influence on the dielectric properties, with increased pre-stretch consistently reducing the effective dielectric constant through modification of polymer-chain alignment, specimen thickness, and molecular arrangement. This effect is strongly material-dependent: increasing the pre-stretch product from 1×2 to 3×4 reduced the dielectric constant of VHB 4910 from 6.27 to 4.23 at 0℃, a decrease of 32.53%, whereas the corresponding reduction for Oppoband 8001 was only 14.23%, from 2.60 to 2.23. The electrostriction constants obtained from the three-dimensional fitting, a = −0.0410 for VHB 4910 against −0.0265 for Oppoband 8001, quantify this contrast, as do the temperature coefficients b = 603 and 452, respectively. The combined influences of temperature and pre-stretch are linked to strain-induced crystallisation, which can considerably affect the dielectric polarisation properties and result in nonlinear fluctuations in the dielectric constant. Oppoband 8001 displays trends that are generally similar to those of VHB 4910, yet its dielectric behaviour above 0◦C varies significantly, a difference that can be ascribed to the inherently distinct molecular architecture and non-polar characteristics of natural rubber-based elastomers. Moreover, at reduced measurement frequencies and temperatures beyond 0℃, a nearly linear correlation between dielectric constant and the inverse of absolute temperature is noted, offering a valuable empirical relationship for characterising temperature-dependent dielectric properties. Subsequent research ought to include the effects of flexible electrode materials and electrode elastomer interfaces while simultaneously varying temperature, frequency, and mechanical pre-stretch. Such thorough characterisation would enhance the dependability and broader applicability of dielectric-property databases and aid in the creation of resilient constitutive and multiphysics models for the design of high-performance dielectric elastomer transducers, soft actuators, artificial muscles, energy harvesters, and electromechanical generators.

Acknowledgement

The authors gratefully acknowledge the Robotics and Automation Laboratory, Department of Mechanical Engineering, Indian Institute of Technology Patna, India, for extending the laboratory facilities and technical support required for the fabrication and characterization of the materials reported in this study. The authors also thank the Central Instrumentation Facility, IIT Patna, for access to the characterization equipment.

Funding

The authors have nothing to report.

Conflicts of Interest

The authors declare no conflicts of interest.

Data Availability Statement

The datasets generated and analysed during the current study are available from the corresponding author on reasonable request.

Ethics Approval Statement

Ethical approval was neither required nor sought for this study, as the research was confined to the preparation, processing and characterization of electroactive polymer materials. No human participants, animals, human or animal tissues, or biological samples requiring ethical review were involved at any stage of the work.

References

1) Zhang, Q.; Yu, W.; Zhao, J.; Meng, C.; Guo, S. A review of the applications and challenges of dielectric elastomer actuators in soft robotics. Machines 2025, 13 (2), 101.

(2) Bezsudnov, I. V.; Khmelnitskaia, A. G.; Kalinina, A. A.; Ponomarenko, S. A. Dielectric elastomer actuators: materials and design. Russ. Chem. Rev. 2023, 92 (2).

(3) Liu, L.; Zhang, K.; Liu, J.; Zhu, L.; Xie, R.; Lv, S. Significant improvements in the electromechanical performance of dielectric elastomers by introducing ternary dipolar groups. React. Funct. Polym. 2022, 172, 105177.

(4) Li, S.; Gao, Z.; Yang, W.; Wang, R.; Zhang, L. Recent advances in dielectric elastomer actuator-based soft robots: classification, applications, and future perspectives. Gels 2025, 11 (11), 844.

(5) Xi, S.; Yang, S.; Xiang, C.; Chen, Y.; Niu, Y.; Yang, J.; He, X. Advancements and challenges in dielectric elastomer actuator-based biomimetic mobile robots. Sens. Actuators, A 2024, 380, 116024.

(6) Kurata, H.; Wiranata, A.; Maeda, S.; Cava, D. G.; Giorgio-Serchi, F.; Hosoya, N. Dynamic response characterization of soft fluidic actuators via dielectric elastomer sensors. Measurement 2025, 246, 116616.

(7) Wang, Z.; Xu, Q.; Zhou, Y.; Zhu, Z.; He, B. Modeling of temperature effect on electromechanical properties of dielectric elastomer minimum energy structures. Int. J. Non-Linear Mech. 2024, 159, 104596.

(8) Guo, Y.; Liu, L.; Liu, Y.; Leng, J. Review of dielectric elastomer actuators and their applications in soft robots. Adv. Intell. Syst. 2021, 3 (10), 2000282.

(9) Guo, Y.; Qin, Q.; Han, Z.; Plamthottam, R.; Possinger, M.; Pei, Q. Dielectric elastomer artificial muscle materials advancement and soft robotic applications. SmartMat 2023, 4 (4), No. e1203.

(10) Shi, Y.; Askounis, E.; Plamthottam, R.; Libby, T.; Peng, Z.; Youssef, K.; Pu, J.; Pelrine, R.; Pei, Q. A processable, high-performance dielectric elastomer and multilayering process. Science 2022, 377 (6602), 228–232.

(11) Kelley, C. R.; Kauffman, J. L. Towards wearable tremor suppression using dielectric elastomer stack actuators. Smart Mater. Struct. 2021, 30 (2), 025006.

(12) Novelli, G. L.; Vargas, G. G.; Andrade, R. M. Dielectric elastomer actuators as artificial muscles for wearable robots. J. Intell. Mater. Syst. Struct. 2023, 34 (9), 1007–1025.

(13) Chen, Y.; Zhao, H.; Mao, J.; Chirarattananon, P.; Helbling, E. F.; Hyun, N. s. P.; Clarke, D. R.; Wood, R. J. Controlled flight of a microrobot powered by soft artificial muscles. Nature 2019, 575, 324–329.

(14) O'Brien, B. M.; Calius, E. P.; Inamura, T.; Xie, S. Q.; Anderson, I. A. Dielectric elastomer switches for smart artificial muscles. Appl. Phys. A 2010, 100, 385–389.

(15) Biddiss, E.; Chau, T. Dielectric elastomers as actuators for upper limb prosthetics: challenges and opportunities. Med. Eng. Phys. 2008, 30, 403–418.

(16) Chakraborti, P.; Toprakci, H. A. K.; Yang, P.; Di Spigna, N.; Franzon, P.; Ghosh, T. A compact dielectric elastomer tubular actuator for refreshable braille displays. Sens. Actuators, A 2012, 179, 151–157.

(17) Wang, Z.; Tang, C.; Wang, Y.; Zhou, L.; Dong, X.; Jiang, S.; Pan, Y.; Liu, X.-J.; Zhao, H. Enhancing the energy conversion efficiency of dielectric elastomer generators via elastic energy storage and recovery. Appl. Energy 2025, 379, 124854.

(18) Gurjar, K. V. S.; Sadangi, A. S.; Kumar, A.; Ahmad, D.; Patra, K.; Collins, I.; Hossain, M.; Ajaj, R. M.; Zweiri, Y. Dielectric elastomer generators: recent advances in materials, electronic circuits, and prototype developments. Adv. Energy Sustainability Res. 2025, 6 (1), No. 2400221.

(19) Liu, L.; Liu, Y.; Leng, J. Theory progress and applications of dielectric elastomers. Int. J. Smart Nano Mater. 2013, 4, 199–209.

(20) O'Halloran, A.; O'Malley, F.; McHugh, P. A review on dielectric elastomer actuators, technology, applications, and challenges. J. Appl. Phys. 2008, 104.

(21) Xue, Z.; Song, H.; Rogers, J. A.; Zhang, Y.; Huang, Y. Mechanically-guided structural designs in stretchable inorganic electronics. Adv. Mater. 2020, 32 (15), 1902254.

(22) Li, J.; Liu, L.; Sun, W.; Zhang, J. The dissipative dynamic performances of dielectric elastomer actuator with viscoelastic effects. Mater. Res. Express 2022, 9 (7), 075701.

(23) Zhao, D.; Yin, Y.; Du, H.; Liu, J. Vibration investigation of conical dielectric elastomer thin membrane for energy harvesting system. J. Sound Vib. 2024, 568, 118073.

(24) Wang, Z.; Xu, Q.; Zhou, Y.; Li, G.; He, B. Effect of temperature and pre-stretch on the dynamic performance of dielectric elastomer minimum energy structure. Sci. Rep. 2024, 14 (1), 15411.

(25) Kumar, A.; Ahmad, D.; Patra, K. Dependence of actuation strain of dielectric elastomer on equi-biaxial, pure shear and uniaxial modes of pre-stretching. IOP Conf. Ser.: Mater. Sci. Eng. 2018, 310, No. 012104.

(26) Shian, S.; Diebold, R. M.; Clarke, D. R. Tunable lenses using dielectric elastomer actuators. Opt. Express 2015, 21 (7), 8669–8676.

(27) Ahmad, D.; Patra, K. Experimental and theoretical analysis of laterally pre-stretched pure shear deformation of dielectric elastomer. Polym. Test. 2019, 75, 291–297.

(28) Wissler, M.; Mazza, E. Electromechanical coupling in dielectric elastomer actuators. Sens. Actuators, A 2007, 138, 384–393.

(29) Tröls, A.; Kogler, A.; Baumgartner, R.; Kaltseis, R.; Keplinger, C.; Schwödiauer, R.; Graz, I.; Bauer, S. Stretch dependence of the electrical breakdown strength and dielectric constant of dielectric elastomers. Smart Mater. Struct. 2013, 22.

(30) Jean-Mistral, C.; Sylvestre, A.; Basrour, S.; Chaillout, J. J. Dielectric properties of polyacrylate thick films used in sensors and actuators. Smart Mater. Struct. 2010, 19.

(31) Yu, L.; Hu, T.; Yang, D.; Wei, Q. Enhanced electromechanical performance of natural rubber dielectric elastomers achieved by in situ synthesis of silver nanoparticles on TiO2 nanoparticles. IET Nanodielectr. 2022, 5 (1), 39–49.

(32) Alam, M. N.; Kumar, V.; Jeong, T.; Park, S.-S. Fabrication of high-performance natural rubber composites with enhanced filler–rubber interactions by stearic acid-modified diatomaceous earth and carbon nanotubes for mechanical and energy harvesting applications. Polymers 2023, 15 (17), 3612.

(33) [Author list not provided in source — verify against DOI]. Improved actuation performance and dielectric strength of natural rubber composites by introducing covalent bonds between dielectric filler and polymeric chains. Polymer 2022, 256, 125273.

(34) [Author list not provided in source — verify against DOI]. Electromechanical performance of dielectric elastomer composites: modeling and experimental characterization. Int. J. Solids Struct. 2023, 281, 112489.

(35) Vertechy, R.; Fontana, M. Electromechanical characterization of a new synthetic rubber membrane for dielectric elastomer transducers. Proc. SPIE 2015, 9430, No. 94300K.

(36) Chen, Y.; Lorenzo, A.; Moretti, G.; Fontana, M.; Vertechy, R. Dielectric elastomer materials for large-strain actuation and energy harvesting: a comparison between styrenic rubber, natural rubber, and acrylic elastomer. Smart Mater. Struct. 2019, 28, 0–22.

(37) Wang, H.; Yang, L. Dielectric constant, dielectric loss, conductivity, capacitance and model analysis of electronic electroactive polymers. Polym. Test. 2023, 120, 107965.

(38) [Author list not provided in source — verify against DOI]. Frequency-dependent dielectric constant prediction of polymers using machine learning. npj Comput. Mater. 2020, 6 (1), 30–32.

(39) Liu, L.; Liu, Y.; Yu, K.; Leng, J. Thermoelectromechanical stability of dielectric elastomers undergoing temperature variation. Mech. Mater. 2014, 72, 33–45.

(40) Zhang, C.; Wei, W.; Sun, H.; Zhu, Q. Study on the properties of different dielectric elastomers applying to actuators. Sens. Actuators, A 2021, 329, 112806.

(41) Wang, F.; Zhou, W.; He, Y.; Lv, Y.; Wang, Y.; Wang, Z. Synergetic improvement of dielectric properties and thermal conductivity in Zn@ZnO/carbon fiber reinforced silicone rubber dielectric elastomers. Compos., Part A 2024, 181, 108129.

(42) Seibert, H.; Scheffer, T.; Diebels, S. Biaxial testing of elastomers—experimental setup, measurement, and experimental optimisation of specimen's shape. Tech. Mech. 2014, 34, 72–89.

(43) Shi, Y.; Cheng, A.; Dai, P.; Jiao, Y.; Lu, Y.; Guo, Y. Preparation of natural rubber (NR)/ethylene-propylene-diene terpolymer (EPDM) blends by radiation crosslinking and its heat resistance to air aging. J. Radiat. Res. Radiat. Process. 2024, 42 (3), No. 030204.

(44) [Author list not provided in source — verify against DOI]. Effect of proteins on the vulcanized natural rubber crosslinking network structure and mechanical properties. Polymers 2024, 16 (21).

(45) Cataldo, F. Preparation of silica-based rubber compounds without the use of a silane coupling agent through the use of epoxidized natural rubber. Macromol. Mater. Eng. 2002, 287, 348–352.

(46) Mensah, B.; Kang, S. I.; Wang, W.; Nah, C. Effect of graphene on polar and nonpolar rubber matrices. Mech. Adv. Mater. Mod. Process. 2018, 4, 1–12.

(47) Cao, M. S.; Wang, X. X.; Zhang, M.; Cao, W. Q.; Fang, X. Y.; Yuan, J. Variable-temperature electron transport and dipole polarization turning flexible multifunctional microsensor beyond electrical and optical energy. Adv. Mater. 2020, 32, 1–8.

(48) Bower, D. I. An Introduction to Polymer Physics; Cambridge University Press: Cambridge, U.K., 2002.

(49) Lu, T.; Liu, Q.; Xin, S.; Peng, D. Effect of frequency on dielectric properties of TiO2/PDMS dielectric elastomers. Chem. Pap. 2020.

(50) Ahmad, Z. Polymeric Dielectric Materials; IntechOpen: London, 2012.

(51) Zhang, Q.; Chen, X.; Zhang, T.; Zhang, Q. M. Giant permittivity materials with low dielectric loss over a broad temperature range enabled by weakening intermolecular hydrogen bonds. Nano Energy 2019, 64, 103916.

(52) McKeen, L. W. Introduction to Plastics and Polymers; Elsevier: Amsterdam, 2012.

(53) Arayapranee, W.; Rempel, G. L. Effects of polarity on the filler-rubber interaction and properties of silica filled grafted natural rubber composites. J. Polym. 2013, 2013, 1–9.

(54) Li, B.; Chen, H.; Qiang, J.; Hu, S.; Zhu, Z.; Wang, Y. Effect of mechanical pre-stretch on the stabilization of dielectric elastomer actuation. J. Phys. D: Appl. Phys. 2011, 44.

(55) Vu-Cong, T.; Jean-Mistral, C.; Sylvestre, A. Impact of the nature of the compliant electrodes on the dielectric constant of acrylic and silicone electroactive polymers. Smart Mater. Struct. 2012, 21.

(56) Schlögl, T.; Leyendecker, S. A polarisation based approach to model the strain dependent permittivity of dielectric elastomers. Sens. Actuators, A 2017, 267, 156–163.

(57) Kofod, G.; Sommer-Larsen, P.; Kronbluh, R.; Pelrine, R. Actuation response of polyacrylate dielectric elastomers. J. Intell. Mater. Syst. Struct. 2003, 14, 787–793.

(58) Trols, A.; Kogler, A.; Baumgartner, R.; Kaltseis, R.; Keplinger, C.; Schwodiauer, R.; Graz, I.; Bauer, S. Stretch dependence of the electrical breakdown strength and dielectric constant of dielectric elastomers. Smart Mater. Struct. 2013, 22.

(59) Murakami, S.; Senoo, K.; Toki, S.; Kohjiya, S. Structural development of natural rubber during uniaxial stretching by in situ wide angle X-ray diffraction using synchrotron radiation. Polymer 2002, 43, 2117–2120.

(60) Lin, W.; Bian, M.; Yang, G.; Chen, Q. Strain-induced crystallization of natural rubber as studied by high-resolution solid-state 13C NMR spectroscopy. Polymer 2004, 45, 4939–4943.

(61) Sheng, J.; Chen, H.; Li, B.; Wang, Y. Influence of the temperature and deformation-dependent dielectric constant on the stability of dielectric elastomers. J. Appl. Polym. Sci. 2013, 128, 2402–2407.

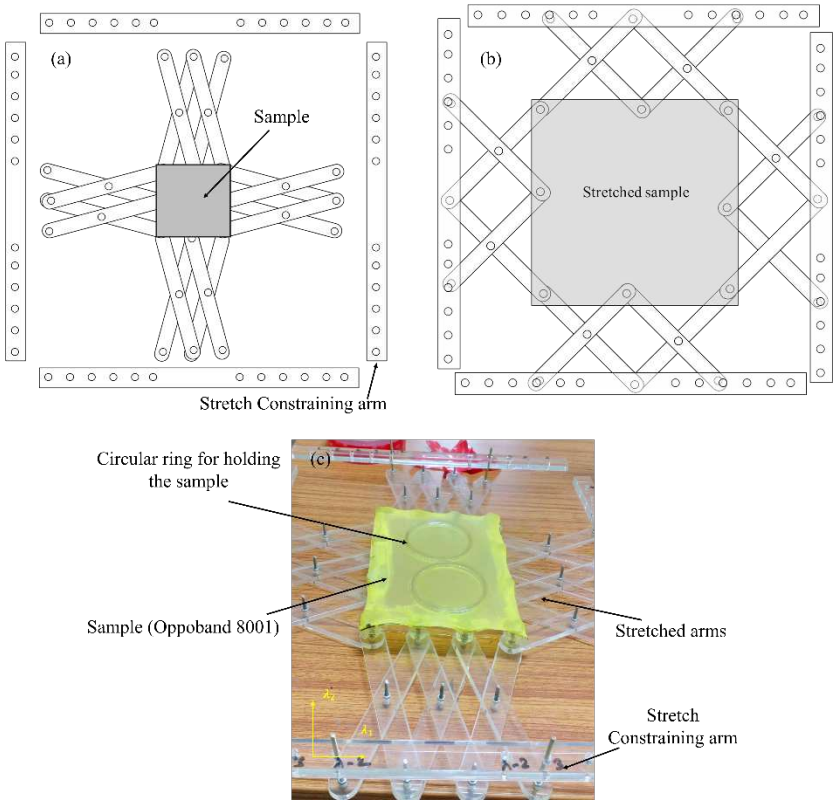


Figure 1: (a), (b)Biaxial stretching device used for pre-stretching the samples, (c) Oppoband equal biaxially stretched

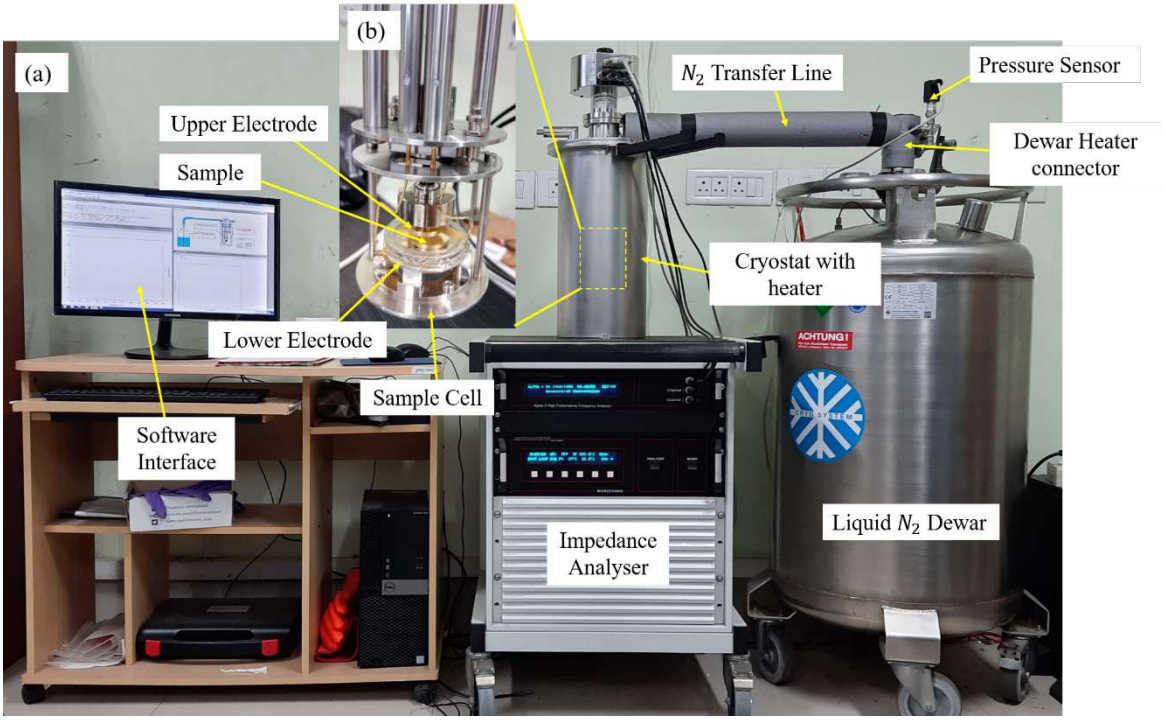


Figure 2: Novocontrol spectroscopy alpha analyzer with high and low temperature controller cryostat chamber along with Liquid nitrogen Dewar

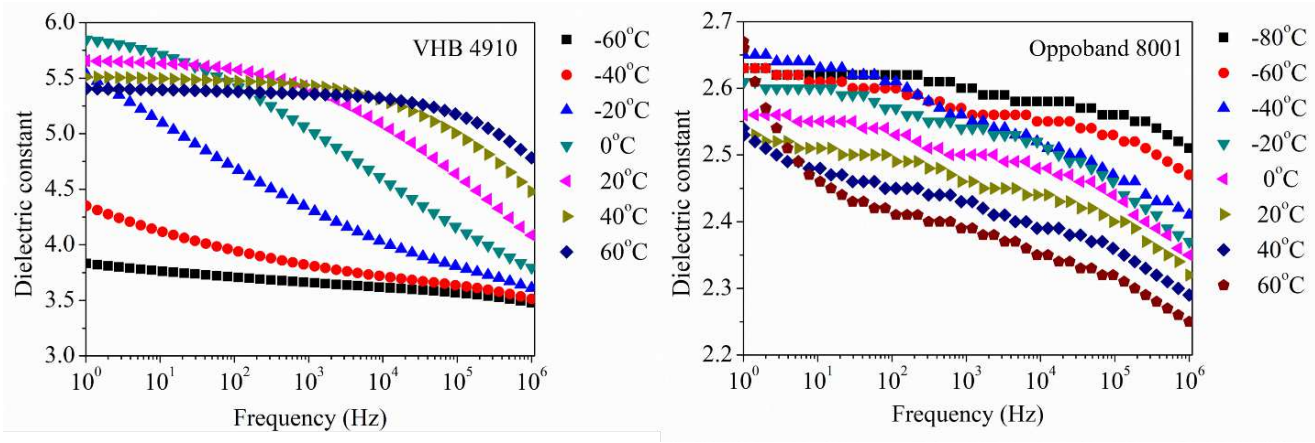


Figure 3: Variation of dielectric constant with frequency range for VHB 4910 and Oppoband 8001 from 1 Hz to 1MHz

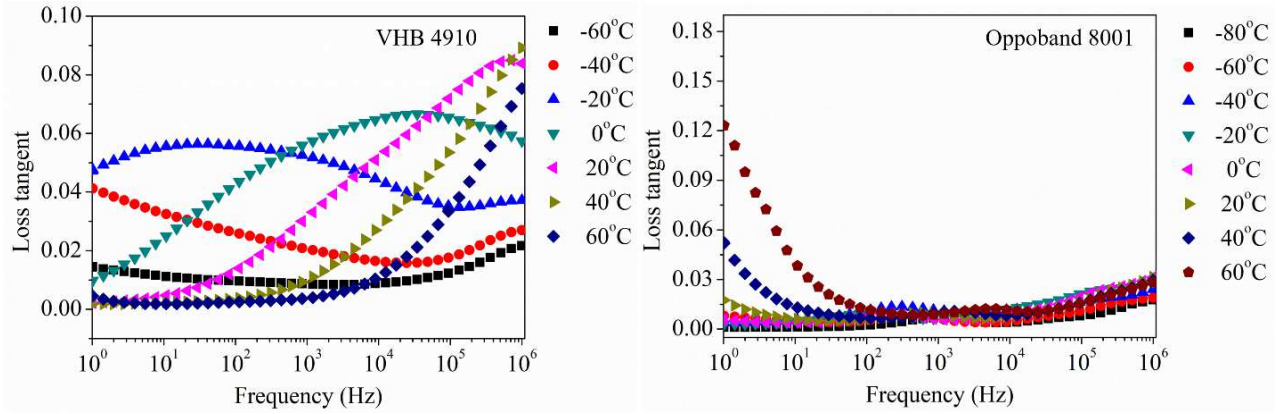


Figure 4: loss tangent variation with frequency of VHB 4910, and Oppoband 8001

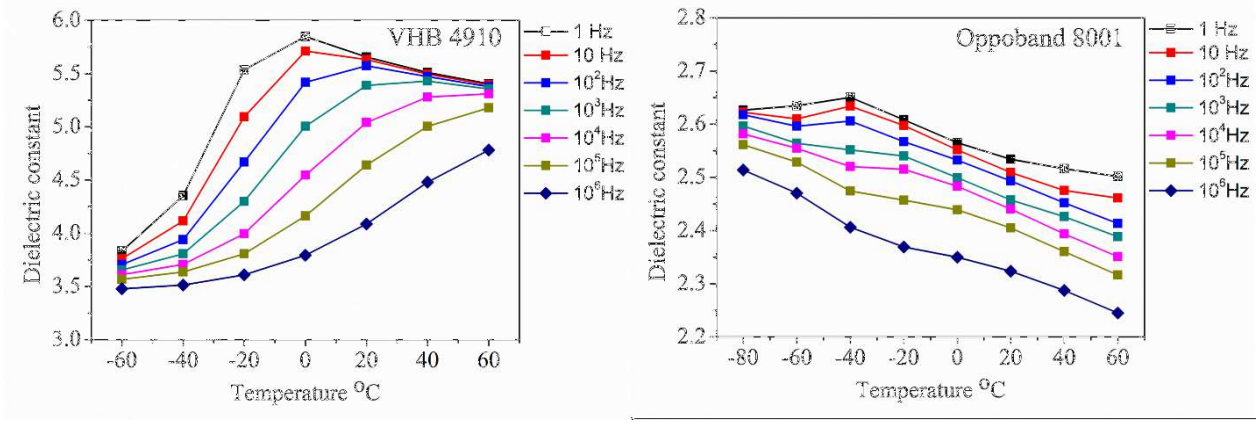


Figure 5: Effect of temperature on dielectric constant of VHB 4910 and Oppoband 8001 at different frequency

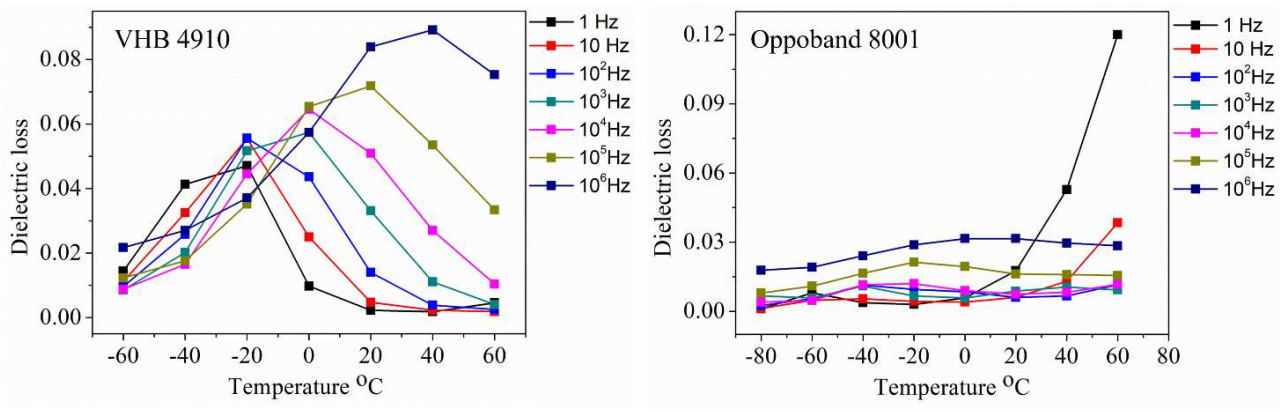


Figure 6: Effect of temperature on dielectric loss of VHB 4910 and Oppoband 8001 at different frequencies and temperature

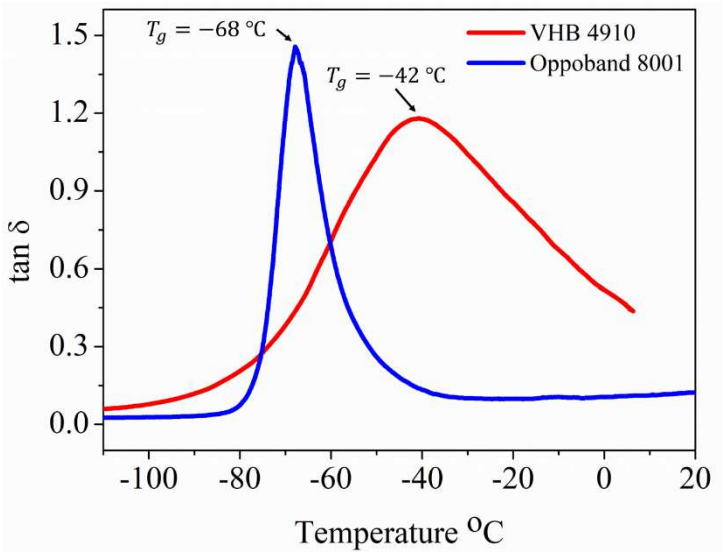


Figure 7: Glass transition temperature of VHB 4910 and Oppoband 8001.

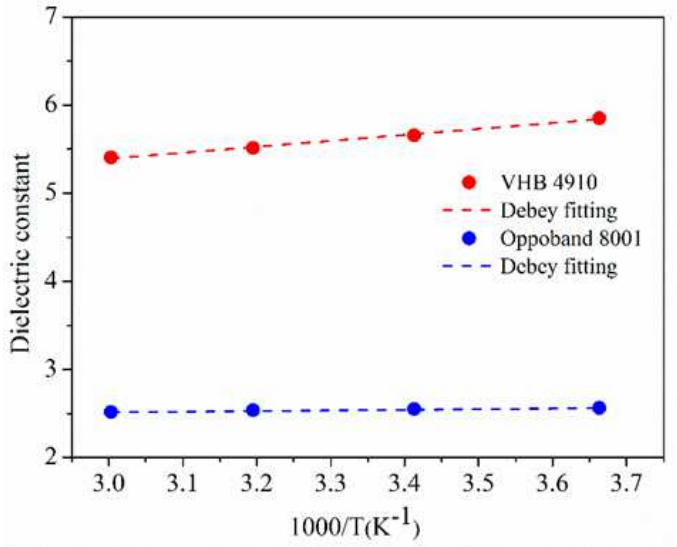


Figure 8: Debye model fitting of VHB 4910 and Oppoband 8001 at 1 Hz.

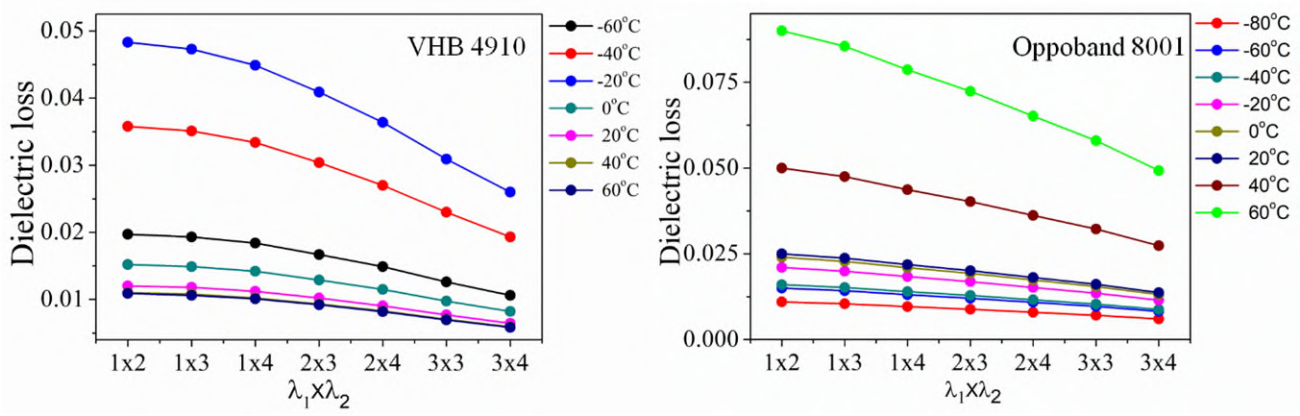


Figure 9: Effect of stretch on dielectric loss (1 Hz) of VHB 4910 and Oppoband 8001 at different temperature.

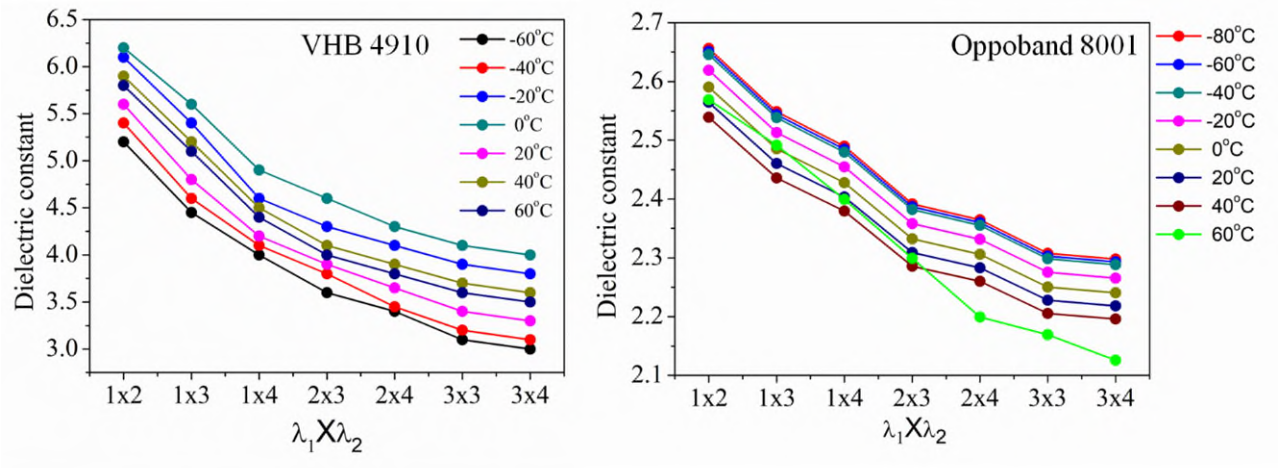


Figure 10: Variation of the dielectric constant for VHB 4910 and Oppoband 8001 at 1 Hz with effect of stretch

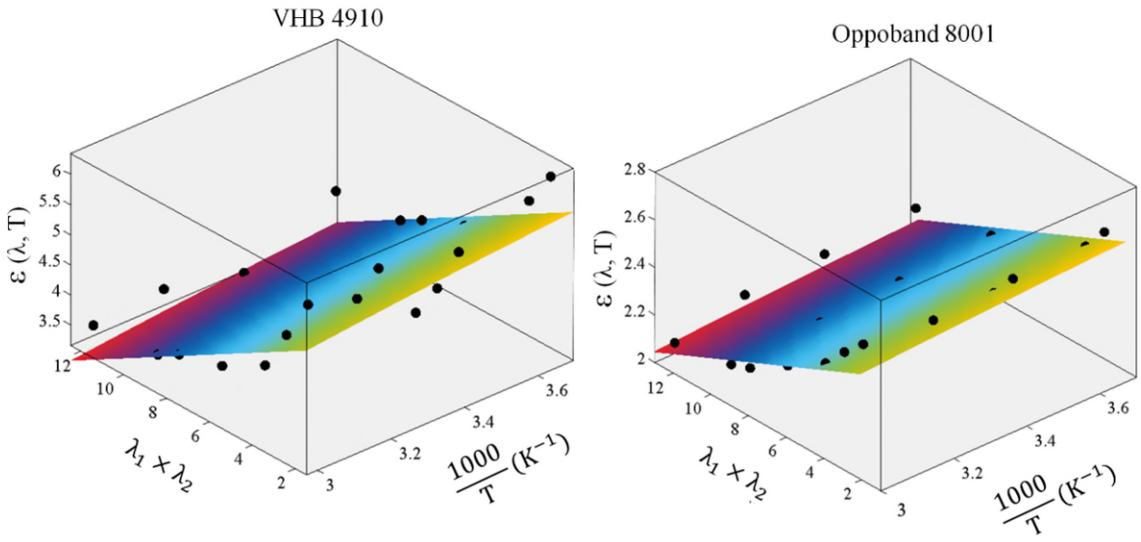


Figure 11: 3D curve fitting of dielectric constant as a function of pre-stretch and temperature based on equation 3 Form equation (3), temperature is inversely proportional to the dielectric constant which indicates that it will decrease an increase of temperature above 0°C also supported by curve fitting shown in figure 8.

Table 1: Details of dielectric elastomers used as EAPs used in this work

Elastomer Type	**Commercial Name**	**Electrode**	**Film Thickness**
Acrylic rubber	VHB 4910	Carbon conductive grease (MG Chemicals)	1 mm
Natural rubber	Oppoband 8001	Carbon conductive grease (MG Chemicals)	150 µm

Table 2: Overview of experimental materials utilised for various stretching modes

Elastomer Type	Stretching Configuration	Prescribed Stretch (λ_1, λ_2)
VHB 4910	Equal-biaxial	(1, 1), (1.25, 1.25), (1.5, 1.5), (1.75, 1.75), (2, 2), (3, 3), (4, 4), (5, 5)
	Samples number	8×3 = 24
	Temperature range (°C)	−60 to 40
	Unequal-biaxial	(2, 3), (2, 4), (2, 5), (3, 4), (3, 5), (4, 5), (2, 1), (3, 1), (4, 1), (5, 1)
	Samples number	10×3 = 30
	Temperature range (°C)	−60 to 40
	Uniaxial	(1.25, 0.89), (1.50, 0.82), (1.75, 0.76), (2, 0.71), (3, 0.58), (4, 0.50), (5, 0.45), (6, 0.41)
	Samples number	8×3 = 24
	Temperature range (°C)	−60 to 40
Oppoband 8001	Equal-biaxial	(1, 1), (1.5, 1.5), (2, 2), (3, 3), (4, 4)
	Samples number	5×3 = 15
	Temperature range (°C)	−80 to 40
	Unequal-biaxial	(2, 3), (2, 4), (2, 1), (3, 1), (4, 1), (5, 1)
	Samples number	6×3 = 18
	Temperature range (°C)	−80 to 40
	Uniaxial	(1.25, 0.89), (1.5, 0.82), (1.75, 0.76), (2, 0.71), (3, 0.58), (4, 0.50), (5, 0.45)
	Samples number	7×3 = 21
	Temperature range (°C)	−80 to 40
Total Number of Samples		**132**

Table 3: Percentage change in dielectric constant with change in frequency at different temperatures

Elastomer	**Temperature (°C)**	**Dielectric constant at 1 MHz**	**Dielectric constant at 1 Hz**	**% change in dielectric constant**
VHB 4910	−60	3.48	3.83	9.13
	−40	3.51	4.35	19.32
	−20	3.61	5.53	34.72
	0	3.79	5.84	35.10
	20	4.09	5.65	27.61
	40	4.48	5.51	18.69
	60	4.78	5.40	11.48
Oppoband 8001	−80	2.51	2.63	4.56
	−60	2.47	2.63	6.08
	−40	2.41	2.65	9.06
	−20	2.37	2.61	9.20
	0	2.35	2.56	8.20
	20	2.32	2.53	8.30
	40	2.29	2.54	9.84
	60	2.25	2.67	15.73

Table 4: Percentage change in dielectric constant with change in frequency at different temperatures

Elastomer	Temperature (°C)	Dielectric constant at ($\lambda_1 \times \lambda_2$)		% change in dielectric constant
		1×2	3×4	
VHB 4910	−60	5.20	3.11	40.19
	−40	5.42	3.06	43.50
	−20	6.15	3.89	36.75
	0	6.27	4.23	32.53
	20	5.68	3.34	41.20
	40	5.92	3.68	37.84
	60	5.83	3.57	38.76
Oppoband 8001	−80	2.66	2.31	13.15
	−60	2.65	2.29	13.58
	−40	2.63	2.27	13.69
	−20	2.61	2.25	13.79
	0	2.60	2.23	14.23
	20	2.58	2.21	14.34
	40	2.56	2.19	14.45
	60	2.53	2.18	13.84

Table 5: Fitting constant of the 3D fitting of dielectric constant on the basis of equation 5

Dielectric elastomer	Fitting constant a	Fitting constant b	Fitting constant c
VHB 4910	−0.0410	603	3.610
Oppoband 8001	−0.0265	452	1.529